

Supplementary Material

Modelling supraglacial debris-cover evolution from the single glacier
to the regional scale: an application to High Mountain Asia

Loris Compagno^{1,2}, Matthias Huss^{1,2,3}, Evan Stewart Miles², Michael James McCarthy², Harry
Zekollari^{4,5,1,2}, Francesca Pelliciotti², Daniel Farinotti^{1,2}.

¹Laboratory of Hydraulics, Hydrology and Glaciology (VAW), ETH Zurich, Zurich, Switzerland

²Swiss Federal Institute for Forest, Snow and Landscape Research (WSL), Birmensdorf, Switzerland

³Department of Geosciences, University of Fribourg, Fribourg, Switzerland

⁴Department of Geoscience and Remote Sensing, Delft University of Technology, Netherlands

⁵Laboratoire de Glaciologie, Université libre de Bruxelles, Belgium

Correspondence: Loris Compagno <compagno@vaw.baug.ethz.ch>

1 This Supplementary Material consist of (i) a Supplementary Method, (ii) Supplementary Results,
2 (iii) a Supplementary Discussion section, (iv) 11 Figures and (v) 1 Table.

3 **S1 Supplementary Methods**

4 **S1.1 2-D interpolation of the results**

5 In Figures 9, S4 and S5, a graphical 2-dimensional extrapolation of the 1-dimensional modelled
6 results is shown. This extrapolation is not physical-based, but is instead a geometrical extrapolation
7 based on the RGI glacier extent. The 2-D images illustrate how glaciers (both glacier geometry
8 and debris cover) could look in the future.

9 The extrapolation method works as follows: for each elevation band, the plotted ice and debris
10 covered area correspond to the the modelled results by adapting the plotted glacier and debris
11 width on that elevation band, where the 'redistribution' starts from the centre of the elevation
12 band.

13 **S2 Supplementary Results**

14 In Addition to Langtang Glacier (Fig. 9 in main manuscript), here we also analyse the evolution
15 of Baltoro Glacier (Fig. S4) and Inylcheck Glacier (Fig. S5).

16 Baltoro Glacier - like Langtang Glacier - shows a slower retreat when debris is explicitly accounted
17 for compared to the simulations where debris is modelled implicitly. By the end of the century
18 and according to the medium emission scenario SSP245, the glacier retreat difference between the
19 explicitly and implicitly modelling debris reaches more than 15 km (Fig. S4a-c) by the end of
20 the 21st century. The modeled fraction of the debris covered area is expected to increase from
21 $25\pm 1\%$ in 2020 to between $27\pm 3\%$ (SSP119) and $38\pm 8\%$ (SSP585) in 2100 (Fig. S4d). For the
22 same time period (i.e. between 2020 and 2100), the mean debris thickness is projected to increase
23 between $35\pm 12\%$ (SSP119) and $140\pm 85\%$ (SSP585) (Fig. S4g). This significant debris thickness
24 increase is due to the long-term negative mass balance and today's thick debris cover (mean of
25 40 cm for the 2000-2016 reference period). Baltoro Glacier will lose between $24\pm 17\%$ (SSP119)
26 and $53\pm 26\%$ (SSP585) of its 2020 ice volume by 2100 when modelling debris explicitly (Fig. S4e).
27 The numbers change to between $30\pm 28\%$ (SSP119) and $70\pm 20\%$ (SSP585) when modelling debris
28 implicitly (Fig. S4f). Similar differences are obtained when comparing the evolution of the glacier
29 area with and without explicit representation of debris cover (Fig. S4h - i). This results shows the
30 importance of explicitly modelling debris and its evolution.

31 Inylcheck Glacier has less debris cover compared to Langtang and Baltoro Glacier (both in terms
32 of debris covered area fraction and mean thickness). The fraction of the debris-covered area is
33 $22\pm 1\%$ in 2020, and is projected to change to between $21\pm 2\%$ (SSP119) and $44\pm 8\%$ (SSP585)
34 by the end of the century (vs. 2020). The mean debris thickness is projected to change between
35 $-29\pm 1\%$ (SSP119) and $+35\pm 13$ (SSP585). The expected mean debris thickness decrease with low

36 SSPs (SSP119 and SSP126) is attributed to the loss of the frontal ca. 5 km of ice, which is covered
37 by 0.5-0.8 m of debris, and which cannot be counterbalanced by the debris thickness increase of the
38 up-glacier debris-covered areas of the glacier (which occurs under the warmer SSPs, see Fig. S5a-c).
39 Due to the fact that Inylcheck Glacier has a small debris covered area fraction and generally thin
40 debris thickness, the difference in geometry and therefore in volume and area evolution is relatively
41 limited. Indeed, by 2100, Inylcheck Glacier is anticipated to lose between $16\pm 2\%$ (SSP119) and
42 $62\pm 11\%$ (SSP585) of its 2020 ice volume when accounting for debris explicitly, and between $17\pm 8\%$
43 (SSP119) and $61\pm 10\%$ (SSP585) of its 2020 ice volume when using the implicit approach.

44 S3 Supplementary Discussion

45 S3.1 Glacier specific studies

46 Until now, only few studies have implemented in their model a time-dependent debris-cover evolu-
47 tion module (e.g. Jouvét et al., 2011; Rowan et al., 2015; Kienholz et al., 2017; Verhaegen et al.,
48 2020). Despite that three of the four above-cited studies focus on glaciers outside the HMA region,
49 here we qualitatively compare our methodology and results with those of the above cited studies.
50 The aim of this section is to show that, in general, our debris evolution module has similarities
51 with previous higher-order approaches, and that our debris evolution projections are in line with
52 previous findings.

53 Jouvét et al. (2011) modelled the debris evolution of Grosser Aletschgletscher, Switzerland, ini-
54 tialising their model with observations of spatial debris distribution. In their model, debris-front
55 propagates in the outward normal direction, and the debris divergence speed is prescribed by the
56 mass balance and by a calibration parameter. This method is similar to our debris lateral expan-
57 sion parametrization. The simulation showed that Grosser Aletschgletscher - which has two central
58 moraines and a debris-cover of only 4% in 2010 - can significantly gain debris with time, so that
59 by 2100, depending on the calibration parameter, it could become a full debris-covered tongue.
60 This significant debris-cover increase is also simulated on HMA glaciers using our module. E.g.
61 for Kangjiaruo Glacier (which today has a debris-covered area of 14%), debris covered fraction is
62 modelled to increase in the future, resulting in a completely debris covered glacier tongue.

63 Herreid and Pellicciotti (2020) also described such a significant potentially increase in the debris
64 covered fraction for Kangjiaruo Glaciers and the other HMA glaciers. In a nutshell, Herreid and
65 Pellicciotti (2020) explain that in a warming climate, debris-covered glaciers with remaining de-
66bris expansion potential will gain debris through time, until reaching a glacier-specific maximum
67 amount of debris, which show this hypothesis for Kangjiaruo Glacier, in close correspondence to
68 our own results. However, as a second hypothesis, Herreid and Pellicciotti (2020) also indicate that
69 another possible trajectory consists of a rapid glacier decline that outpaces debris-cover evolution.
70 This second hypothesis is also confirmed by some of our results (e.g. Langtang Glacier). Indeed,
71 especially for high SSPs (e.g. SSP370 and SSP585), glacier shrinkage is faster than the debris
72 lateral expansion and up-glacier migration, resulting in a loss of the debris covered fraction.

73 Rowan et al. (2015) modelled the future evolution of Khumbu Glacier. Debris transport is simulated
74 englacially and supraglacially, so that the feedback between ice flow and mass balance is accounted
75 for. They showed that the debris-cover of Khumbu Glacier will develop on the tongue of the glacier

76 near the upper part of the icefall by the end of the century. Indeed, at present, the icefall divides
77 the debris-covered tongue from the debris-free accumulation area. [Rowan et al. \(2015\)](#) simulated
78 that the debris cover will thicken by around 0.25-0.5 m between 2015 and 2100 across the glacier
79 tongue. Although our method is strongly simplified, we also simulate a debris expansion in the
80 upper part of Khumbu’s Glacier icefall by the end of the century. Additionally, our model also
81 shows a debris thickening by around 0.2 — 0.5 m for the same location and time period as modelled
82 by [Rowan et al. \(2015\)](#).

83 [Kienholz et al. \(2017\)](#) modelled lateral expansion of debris for each elevation band based on a
84 relationship between normalized elevation range and moraine lateral expansion on Black Rapids
85 Glacier (Alaska). Again, our debris lateral expansion method - despite its simplicity - is similar to
86 the author’s method. As a result, [Kienholz et al. \(2017\)](#) showed that the debris-covered fraction of
87 Black Rapids in the future will increase, principally due the debris lateral expansion. Although a
88 direct comparison is not possible, our modelled debris cover evolution is generally comparable with
89 the findings by [Kienholz et al. \(2017\)](#).

90 [Verhaegen et al. \(2020\)](#) modelled the future debris evolution of Djankuat Glacier (Caucasus). The
91 authors simulated the debris lateral expansion through a parametrization based on an exponential
92 relationship between the debris lateral expansion on a specific location on the glacier and its distance
93 from the terminus. Debris thickness is modelled according to melt-out from ice, downstream
94 advection of supraglacial debris and the intake or removal of supraglacial debris from the glacier
95 surface. This relatively sophisticated model needs many input parameters, such as debris input
96 location, the time of release of debris source, and debris flux magnitude (see [Verhaegen et al., 2020](#),
97 for more details). The authors demonstrated that changes in the input parameters, and therefore
98 also accounting for debris-cover explicitly or implicitly, can have important implications in the
99 future evolution of Djankaut Glacier. Similar to [Verhaegen et al. \(2020\)](#), our study shows that the
100 expected evolution of glaciers can differ considerably if debris-cover is accounted for or omitted,
101 and that parameter calibration can strongly influence model results.

102 S4 Supplementary figures

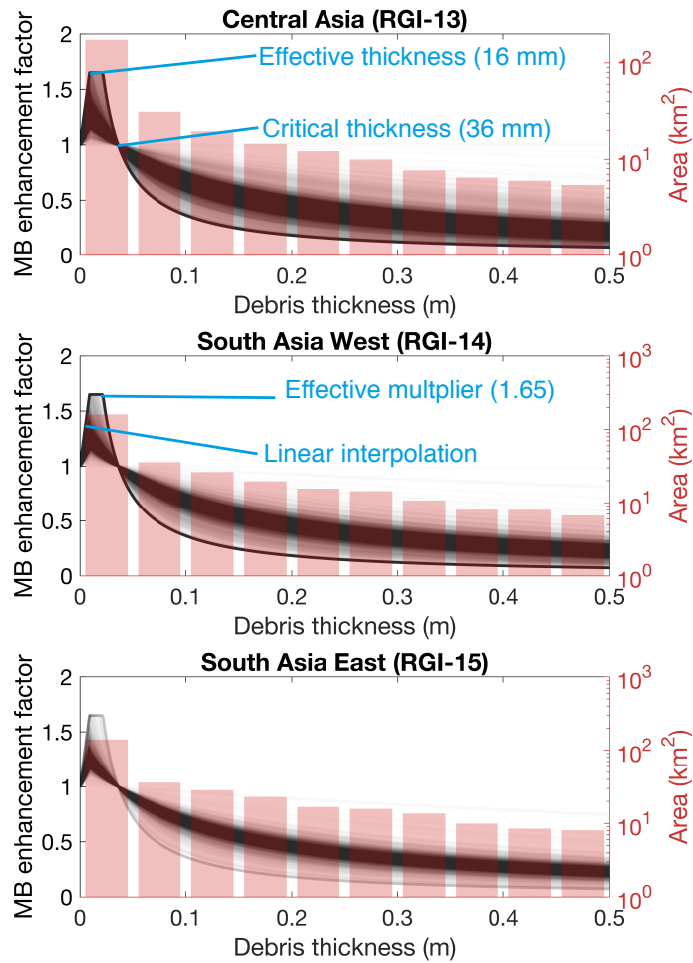


Figure S1: Mass balance (MB) enhancement factor as a function of debris thickness for the three RGI regions considered in this study. For every glacier a semi-transparent black line is plotted. Overlapping lines thus become darker. Each semi-transparent black line corresponds to a glacier specific Østrem-curve. The red bars show debris covered area for a given debris thickness.

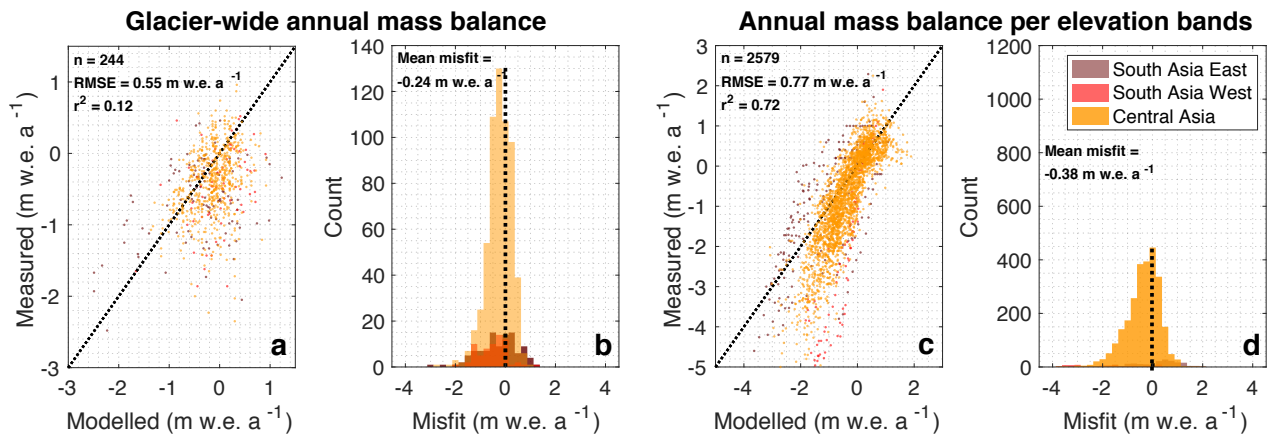


Figure S2: Evaluation of modelled annual glacier-wide and per elevation bands mass balance with observations from 21 glaciers provided by the World Glacier Monitoring Service (WGMS, 2020)

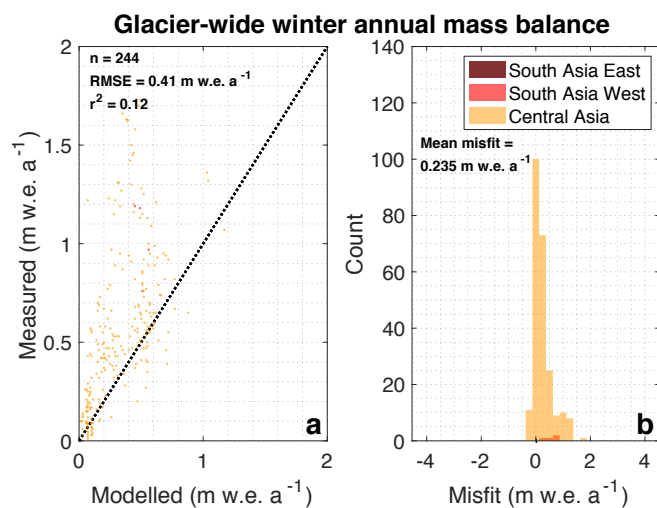


Figure S3: Evaluation of modelled glacier-wide winter mass balance with observations from 21 glaciers provided by the World Glacier Monitoring Service (WGMS, 2020)

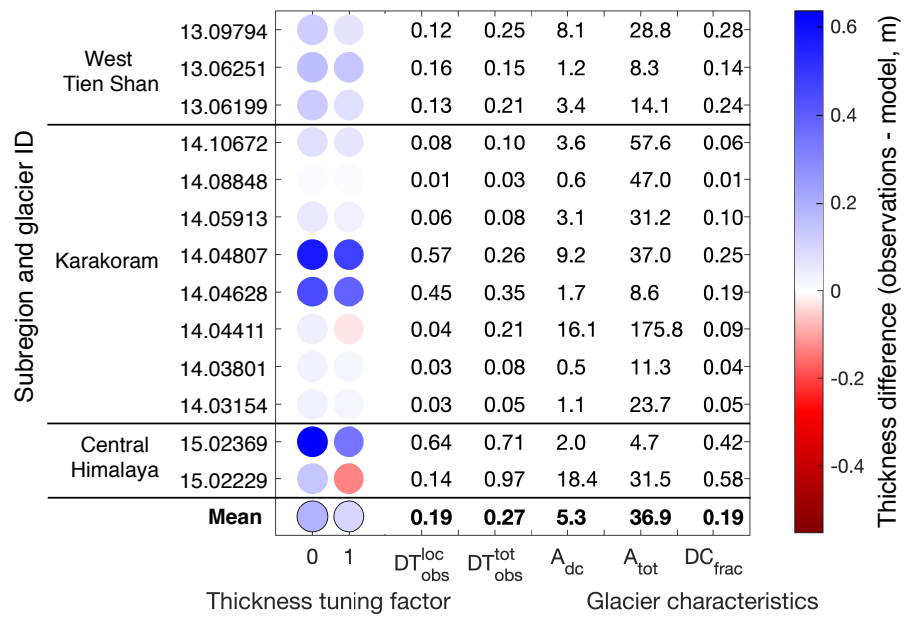


Figure S4: Same as Figure 5, but on glaciers set S2 and using 0 and 1.0 as $c_{thickening}$.

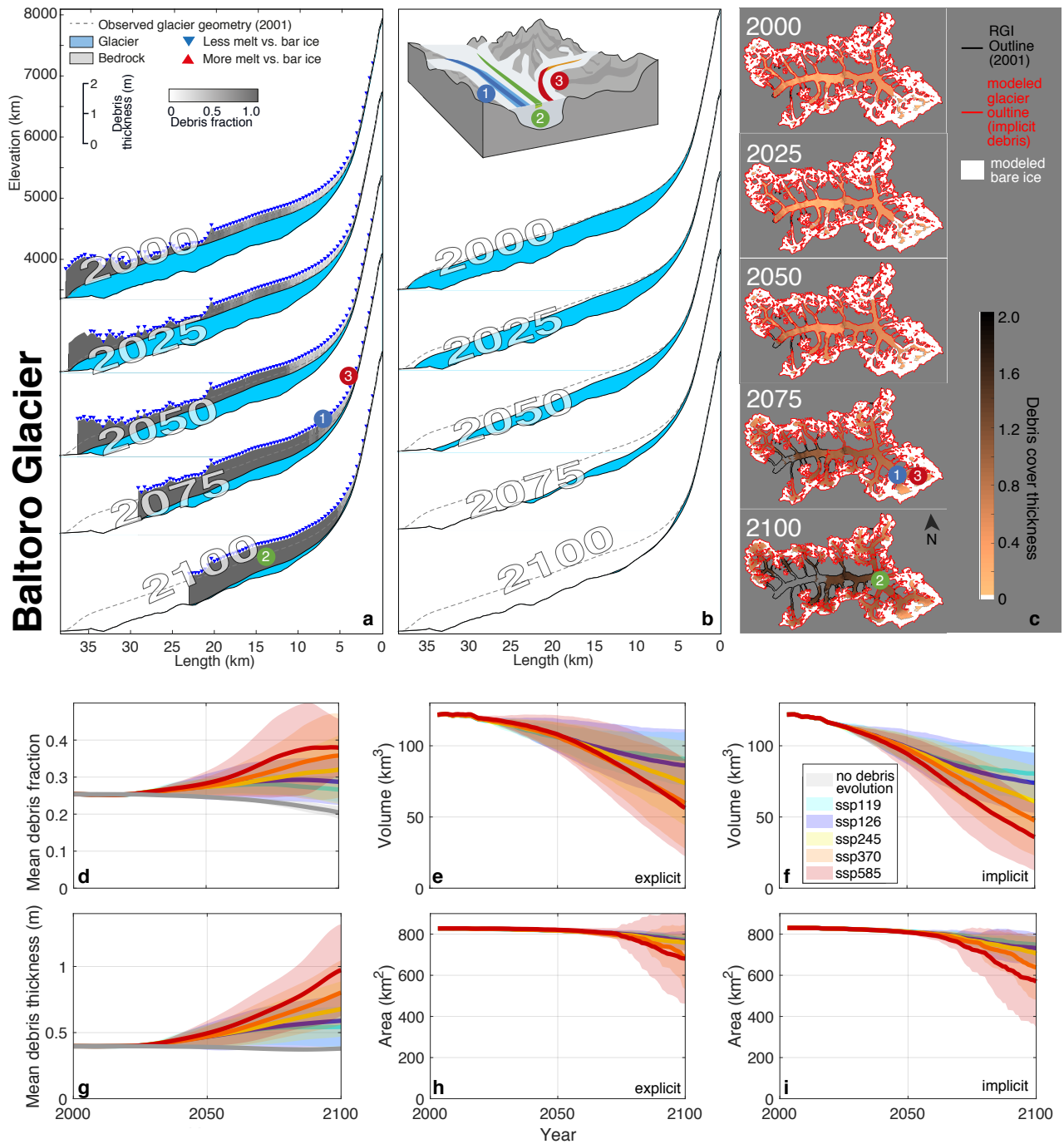


Figure S5: (a) Modelled evolution of Baltoro Glacier when debris is explicitly accounted for. The results refer to SSP245. Note that the debris thickness (grey) is exaggerated by a factor of 500 for visibility. The three parametrizations included in the debris-cover module (cf. section 3.2 and Figure 3) are indicated by the circled, colored numbers, and described in the text. (b) Same as (a), but accounting for debris implicitly, i.e. glacier evolution is not modelled with the new debris module, but by re-calibrating some of the model parameters to match observed long-term mass balance (see section 4.1 for details). (c) Model results extrapolated to 2D (see Supplementary Material for the extrapolation method). For every SSP, the evolution of (d) debris-cover fraction, (e/f) glacier volume with explicit/implicit debris-cover modelling, (g) debris thickness, and (h/i) glacier area with explicit/implicit modelling is shown. The shaded ranges represent one standard deviation of all climate model members included in a given SSP.

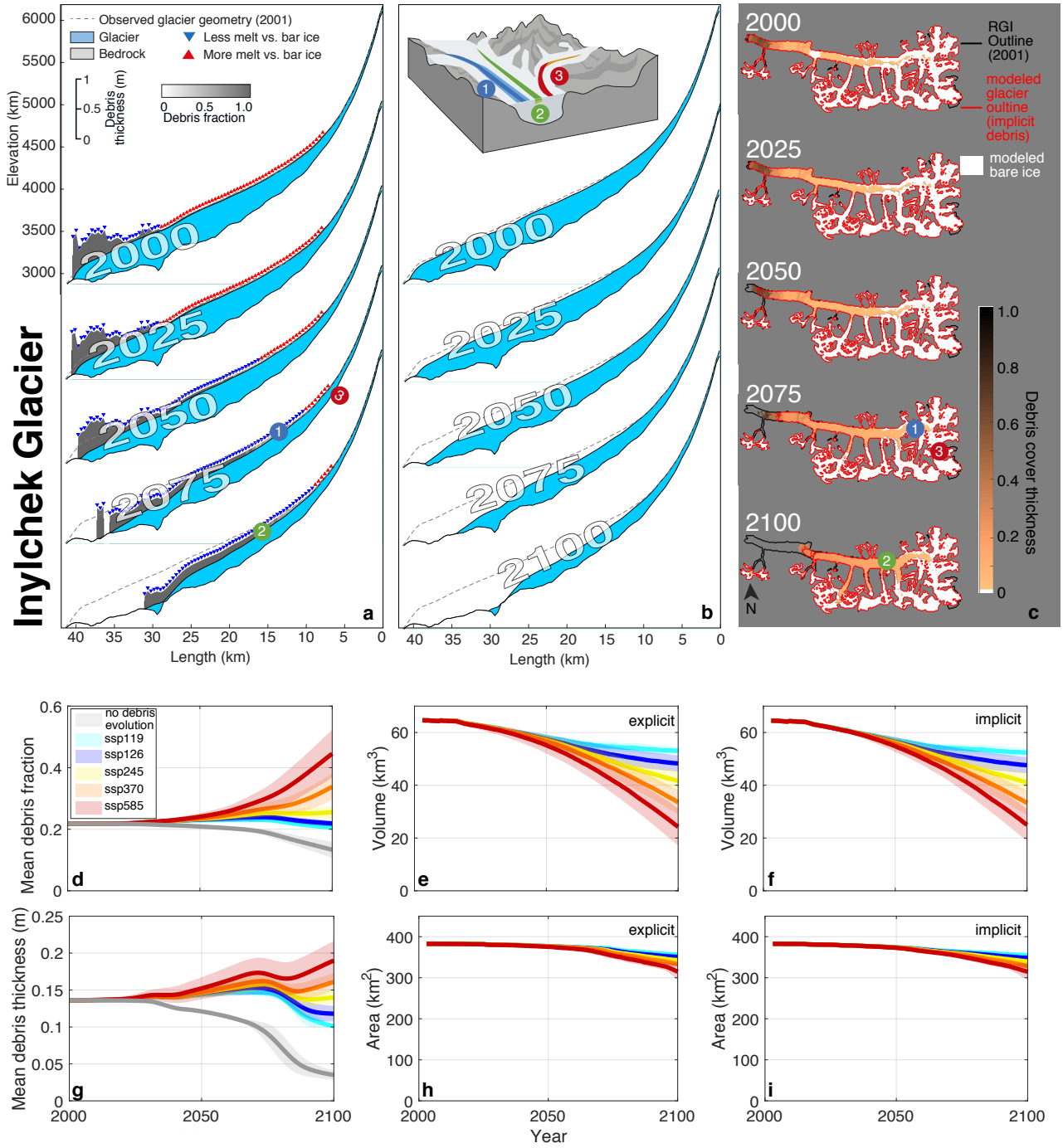


Figure S6: Like S5, but for Inylchek Glacier

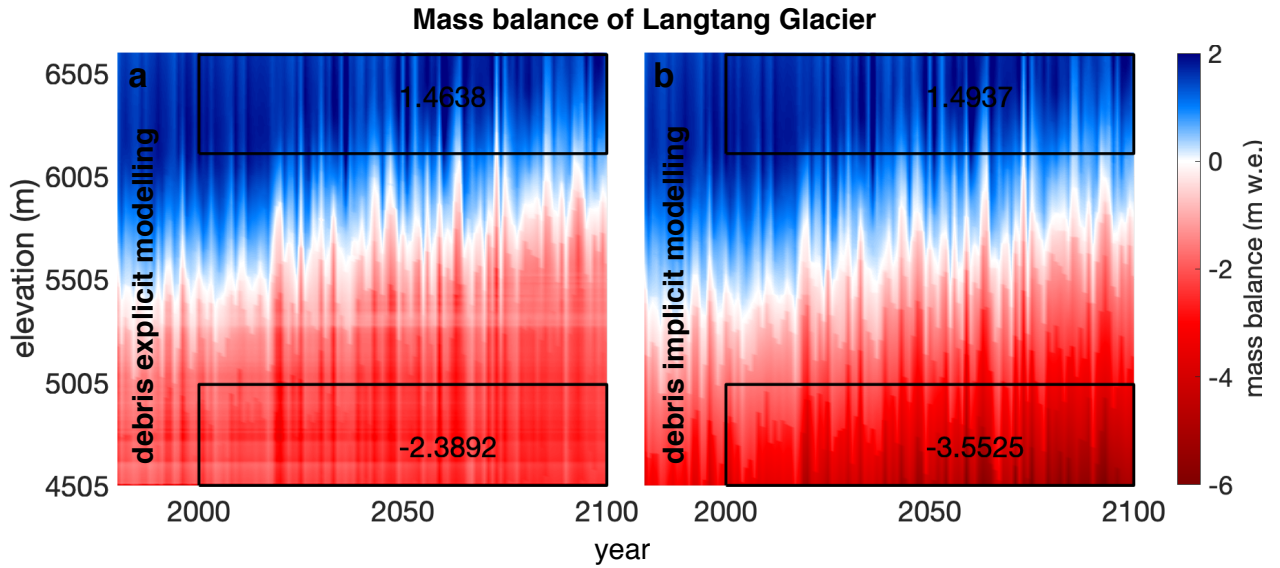


Figure S7: Mass balance evolution of Langtang Glacier with SSP245 when (a) modelling debris explicitly and (b) modelling debris cover implicitly. Note the higher mass balance gradient with elevation of (a).

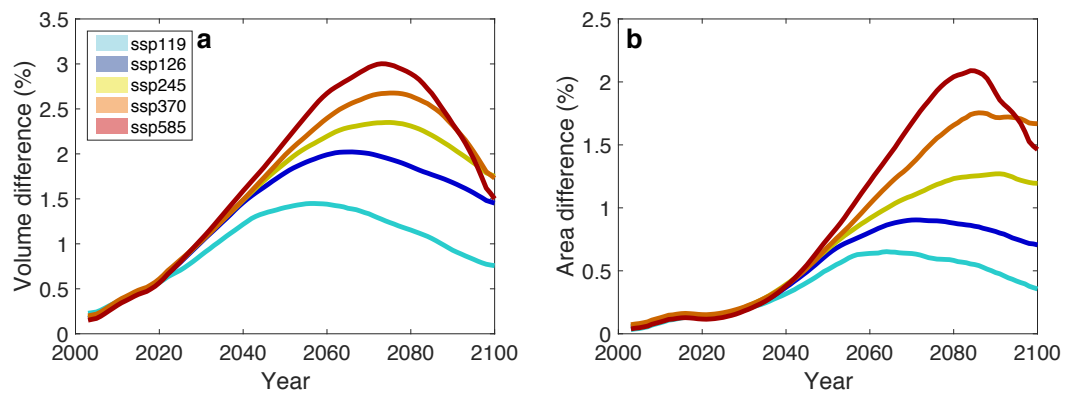


Figure S8: (a) Difference in volume evolution for all glaciers in HMA when modelling debris cover and evolution explicitly vs. implicitly. Positive numbers means that less ice volume is lost when debris cover is explicitly modelled. (b) Like (a), but for the area evolution.

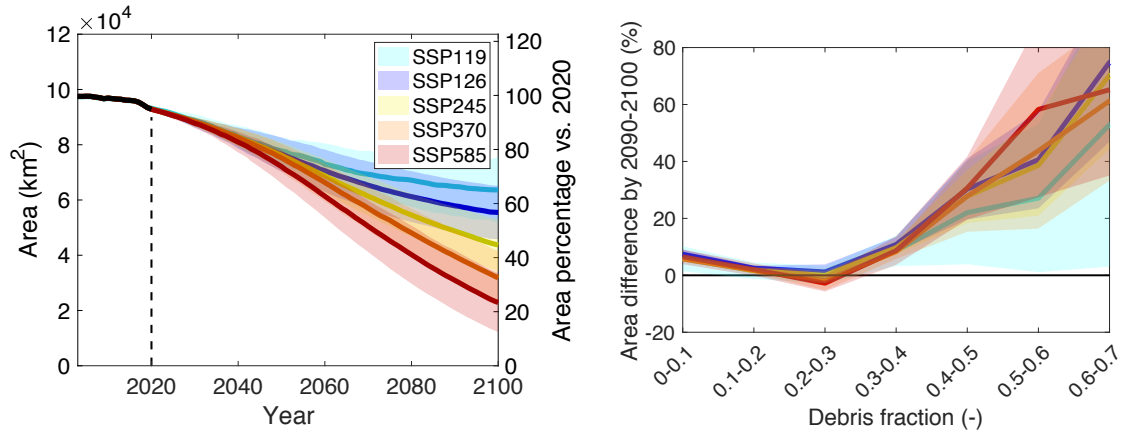


Figure S9: **(a)** Evolution of glacier area for all glaciers in HMA when explicitly modelling debris-cover changes. Results are aggregated to five SSPs **(b)** Difference in area (mean over 2090-2100) between implicit and explicit debris-cover modelling. The shaded bands represent one standard deviation of all climate model members for a given SSP.

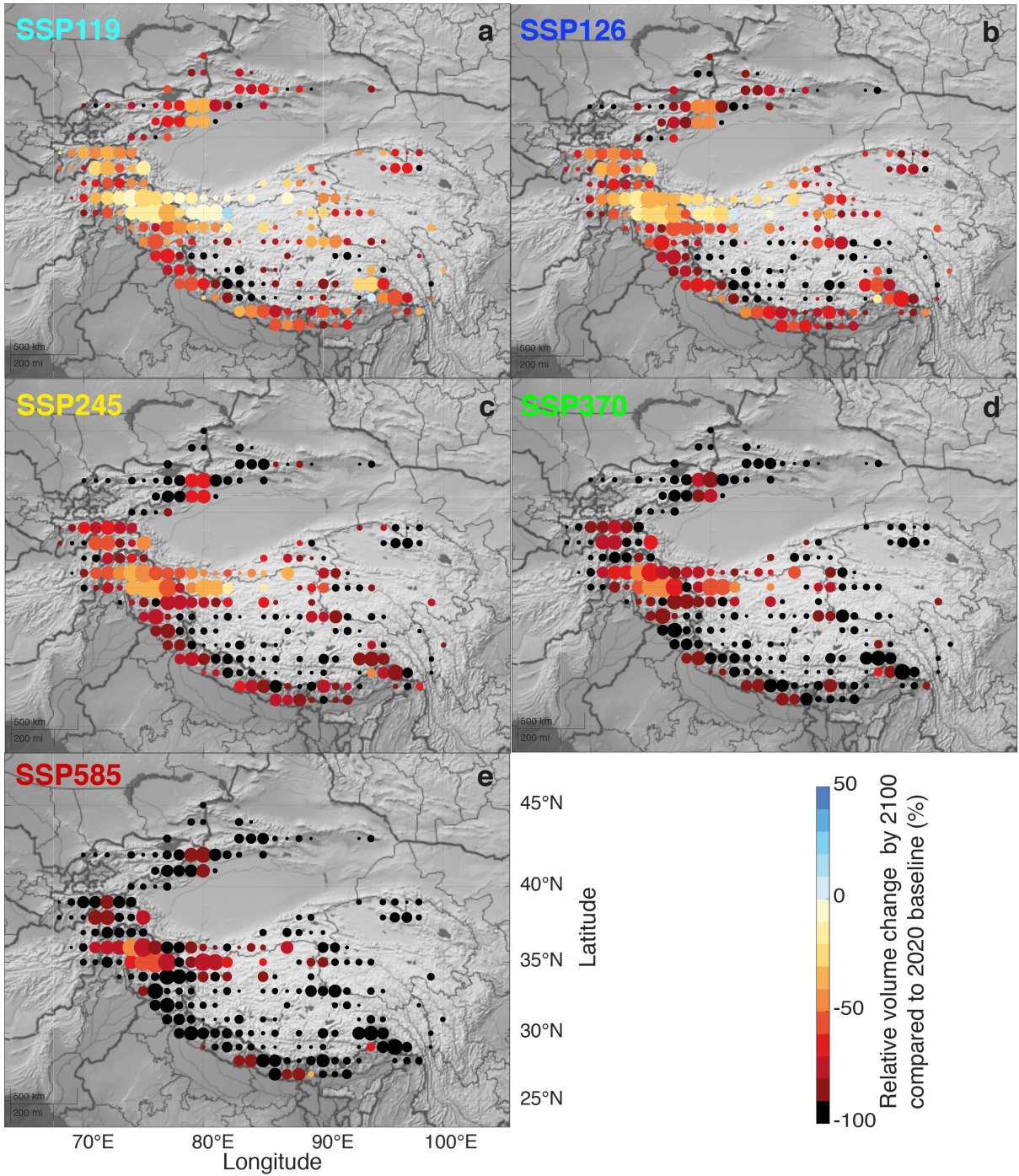


Figure S10: Regional volume evolution of HMA glaciers. The data is divided into a grid with 1° horizontal resolution.

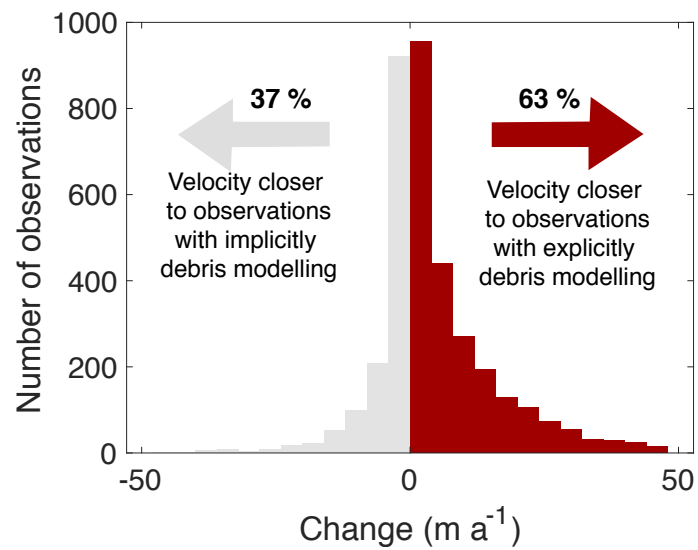


Figure S11: Change of the modelled velocity (m a^{-1}) when modelling debris cover explicitly and implicitly. A positive change means that modelled velocity is closer to the ITS LIVE surface velocity data set (Gardner et al., 2019).

S5 Supplementary Table

103

Table S1: Overview of studies containing value for critical thickness, effective thickness, effective thickness and effective multiplier.

Glacier	Country	Latitude (deg)	Elevation (m.a.s.l.)	Critical thickness (mm)	Effective thickness (mm)	Effective multiplier	Source
Khumbu	Nepal	27.57	5400	50	10	1.6	Kayastha et al. (2000)
Lirung	Nepal	28.13	4400	80	30	2	Tangborn and Rana (2000)
Rakhiot	Pakistan	35.21	3400	30	15	1.62	Mattson and Gardner (1989)
Barpu	Pakistan	36.11	4000	25	18	1.65	Khan (1989)
Baltoro	Pakistan	35.7	3500	20	10	1.36	Mihalcea et al. (2006)
Koxkar	China	41.76	3000	15	14	1.06	Juen et al. (2014)
Batal	India	32.3	4500				Sharma et al. (2016)
Baltoro	Pakistan	35.7	3500	35	15	1.3	Groos et al. (2018)
24K	China	29.7	4000	40	15	1.4	Wei et al. (2010)
Chorabari	India	30.8	4000	30	15	1.32	Dobhal et al. (2013),
Inylchek	Kyrgyzstan	42.16	3000				Hagg et al. (2008)
mean HMA				36	16	1.65	

104 Supplementary References

- 105 Dobhal, D., Mehta, M., and Srivastava, D.: Influence of debris cover on terminus retreat and mass
106 changes of Chorabari Glacier, Garhwal region, central Himalaya, India, *Journal of Glaciology*,
107 59, 961–971, <https://doi.org/10.3189/2013JoG12J180>, 2013.
- 108 Gardner, A. S., Fahnestock, M. A., and Scambos, T. A.: ITS-LIVE Regional Glacier and Ice
109 Sheet Surface Velocities. Data archived at National Snow and Ice Data Center, [https://doi.org/](https://doi.org/10.5067/6II6VW8LLWJ7)
110 10.5067/6II6VW8LLWJ7, 2019.
- 111 Groos, A. R., Mayer, C., Smiraglia, C., Diolaiuti, G., and Lambrecht, A.: A first attempt to model
112 region-wide glacier surface mass balances in the Karakoram: findings and future challenges,
113 *Geografia Fisica e Dinamica Quaternaria*, 40, 137–159, [https://doi.org/10.4461/GFDQ2017.40.](https://doi.org/10.4461/GFDQ2017.40.10)
114 10, 2018.
- 115 Hagg, W., Mayer, C., Lambrecht, A., and Helm, A.: Sub-debris melt rates on southern Inylchek
116 Glacier, central Tian Shan, *Geografiska Annaler: Series A, Physical Geography*, 90, 55–63,
117 <https://doi.org/10.1111/j.1468-0459.2008.00333.x>, 2008.
- 118 Herreid, S. and Pellicciotti, F.: The state of rock debris covering Earth’s glaciers, *Nature Geo-*
119 *science*, 13, 621–627, <https://doi.org/10.1038/s41561-020-0615-0>, 2020.
- 120 Jouvet, G., Huss, M., Funk, M., and Blatter, H.: Modelling the retreat of Grosser Aletschgletscher,
121 Switzerland, in a changing climate, *Journal of Glaciology*, 57, 1033–1045, [https://doi.org/10.](https://doi.org/10.3189/002214311798843359)
122 3189/002214311798843359, 2011.
- 123 Juen, M., Mayer, C., Lambrecht, A., Han, H., and Liu, S.: Impact of varying debris cover thick-
124 ness on ablation: a case study for Koxkar Glacier in the Tien Shan, *The Cryosphere*, 8, 377,
125 <https://doi.org/10.5194/tc-8-377-2014>, 2014.
- 126 Kayastha, R. B., Takeuchi, Y., Nakawo, M., and Ageta, Y.: Practical prediction of ice melting
127 beneath various thickness of debris cover on Khumbu Glacier, Nepal, using a positive degree-day
128 factor, *IAHS-AISH P*, 264, 71–81, 2000.
- 129 Khan, M. I.: Ablation on Barpu Glacier, Karakoram Himalaya, Pakistan a study of melt processes
130 on a faceted, debris-covered ice surface. (MSc thesis, Wilfrid Laurier University.), 1989.
- 131 Kienholz, C., Hock, R., Truffer, M., Bieniek, P., and Lader, R.: Mass Balance Evolution of Black
132 Rapids Glacier, Alaska, 1980 - 2100, and Its Implications for Surge Recurrence, *Frontiers in*
133 *Earth Science*, 5, 56, <https://doi.org/10.3389/feart.2017.00056>, 2017.
- 134 Mattson, L. and Gardner, J.: Energy exchanges and ablation rates on the debris-covered Rakhiot
135 Glacier, Pakistan, *Zeitschrift für Gletscherkunde und Glazialgeologie*, 25, 17—32, 1989.
- 136 Mihalcea, C., Mayer, C., Diolaiuti, G., Lambrecht, A., Smiraglia, C., and Tartari, G.: Ice ablation
137 and meteorological conditions on the debris-covered area of Baltoro glacier, Karakoram, Pakistan,
138 *Annals of Glaciology*, 43, 292–300, <https://doi.org/10.3189/172756406781812104>, 2006.
- 139 Rowan, A. V., Egholm, D. L., Quincey, D. J., and Glasser, N. F.: Modelling the feed-
140 backs between mass balance, ice flow and debris transport to predict the response to cli-
141 mate change of debris-covered glaciers in the Himalaya, *Earth and Planetary Science Let-*
142 *ters*, 430, 427–438, <https://doi.org/10.1016/j.epsl.2015.09.004>, URL [https://linkinghub.](https://linkinghub.elsevier.com/retrieve/pii/S0012821X15005713)
143 [elsevier.com/retrieve/pii/S0012821X15005713](https://linkinghub.elsevier.com/retrieve/pii/S0012821X15005713), 2015.

- 144 Sharma, P., Patel, L. K., Ravindra, R., Singh, A., Mahalinganathan, K., and Thamban, M.: Role
145 of debris cover to control specific ablation of adjoining Batal and Sutri Dhaka glaciers in Chandra
146 Basin (Himachal Pradesh) during peak ablation season, *Journal of Earth System Science*, 125,
147 459–473, <https://doi.org/10.1007/s12040-016-0681-2>, 2016.
- 148 Tangborn, W. and Rana, B.: Mass balance and runoff of the partially debris-covered Langtang
149 Glacier, Nepal, *Iahs Publication*, 264, 99–108, 2000.
- 150 Verhaegen, Y., Huybrechts, P., Rybak, O., and Popovnin, V. V.: Modelling the evolution
151 of Djankuat Glacier, North Caucasus, from 1752 until 2100 CE, *The Cryosphere*, 14, 4039–
152 4061, <https://doi.org/10.5194/tc-14-4039-2020>, URL [https://tc.copernicus.org/articles/
153 14/4039/2020/](https://tc.copernicus.org/articles/14/4039/2020/), 2020.
- 154 Wei, Y., Tandong, Y., Baiqing, X., and Hang, Z.: Influence of supraglacial debris on summer
155 ablation and mass balance in the 24K Glacier, southeast Tibetan Plateau, *Geografiska Annaler:
156 Series A, Physical Geography*, 92, 353–360, <https://doi.org/10.1111/j.1468-0459.2010.00400.x>,
157 2010.
- 158 WGMS: Fluctuations of glaciers database, <https://doi.org/10.5904/wgms-fog-2020-08>, 2020.